EFFECT OF (BIO)SURFACTANT TYPE AND CONCENTRATION ON THE GAS-LIQUID EQUILIBRIUM PARTITIONING OF HYDROPHOBIC VOLATILE ORGANIC COMPOUNDS

Paula Alejandra Lamprea Pineda[a], Kristof Demeestere[a], Max Sabbe[a], Joren Bruneel[b], Herman Van Langenhove[a], Christophe Walgraeve[a]

[a]Research group EnVOC, Department of Green Chemistry and Technology, Faculty of Bioscience Engineering, Ghent University, Coupure Links 653, 9000, Ghent Belgium

[b]Trevi nv, Air Division, Dulle-Grietlaan 17/1, 9050, Ghent, Belgium

Correspondence to: Christophe Walgraeve (Christophe.Walgraeve@UGent.be). Tel: +32 9 264 59 53

Co-authors: PaulaAlejandra.LampreaPineda@UGent.be, Kristof.Demeestere@UGent.be, Sabbe.Max@gmail.com, JBruneel@trevi-env.com, Herman.VanLangenhove@UGent.be, Christophe.Walgraeve@UGent.be.

Abstract

The biological removal of hydrophobic volatile organic compounds (VOCs) is limited by their low water solubility and, therefore, low bioavailability. The addition of surfactants is a promising strategy, but to gain understanding and broaden its applicability, its effect on the solubility of hydrophobic VOCs should be investigated. This study evaluates the effect of 2 synthetic surfactants (sodium dodecyl sulfate (SDS) and Tween 80) and 3 biological surfactants (surfactin, rhamnolipid and saponin) on the gas-to-liquid equilibrium partitioning coefficient (K_{GL}) of 7 hydrophobic VOCs at different critical micelle concentrations (CMC). For all VOCs, a decrease in their K_{GL} was observed when a (bio)surfactant was added at 1 and 3 CMC. The highest decrease in K_{GL} (71 – 96%) was observed for all compounds when SDS was added at 3 CMC, whereas the smallest effect was noticed when Tween 80 or surfactin (5.1 – 75%) were added at both concentrations. The results are explained in terms of the (bio)surfactant and VOC physical-chemical properties (e.g. CMC and polarity). This is the first study evaluating the effect of biological surfactants on K_{GL}. These fundamental data are essential to improve the design and modeling of air treatment systems using (bio)surfactants.

Keywords: hydrophobic VOCs, (bio)surfactants, CMC, gas-liquid partitioning coefficient, gas treatment.

Environmental Implication

The compounds (7) selected in this study pose serious problems to human health and the environment, of which 3 are classified as hazardous air pollutants (EPA). They are normally present in waste gas streams. However, they show low removal performances in biological treatment technologies, mainly due to their low solubility in water and, therefore, low bioavailability for microorganisms. The addition of surfactants is a promising strategy, but to gain an understanding and expand their applicability, the effect of surfactant type and concentration on the solubility of these compounds is of paramount importance.

1. Introduction

Volatile organic compounds (VOCs) are emitted in large quantities worldwide from a broad range of industries including oil and gas, textile, chemical, pharmaceutical and food processing, among others. Their emission can result in negative environmental and health effects. Therefore, stringent regulations have driven the industry to implement technologies to control and reduce the emissions and thus exposure to VOCs (e.g. Directive 2010/75/EU on industrial emissions [1] and 40 CFR, 59 – National volatile organic compound emission standards for consumer and commercial products [2]).

Due to the diversity and wide range of concentrations (up to 100 g m^{-3}) of VOCs present in waste gas streams, a broad range of technologies have been developed [3,4]. They are generally classified as destruction (e.g. oxidation, biofiltration) or recovery-based techniques (e.g. absorption, condensation, membrane separation), and include physical-chemical and/or biological transformations [5,6]. The choice depends mainly on the source, the operating conditions and the pollutant's physical-chemical characteristics. Biotechnologies are of particular interest because of their low energy consumption, low operating costs and minimal generation of by-products [7,8]. The process relies on the ability of microorganisms to degrade the VOCs. The microorganisms grow as a biofilm (composed mainly of water [9]) over a support media or may also be suspended in a liquid phase. Initially, the VOCs present in the air stream must be transferred from the gas into the water phase, after which they are sorbed and/or biodegraded [10,11]. The most successful removal of VOCs in gas-phase bioreactors occurs for highly soluble compounds with low molecular weight [7]. Therefore, gas-phase bioreactors such as biotrickling filters, bioscrubbers and biofilters show low removal performances for hydrophobic VOCs, especially due to their low mass transfer and therefore, low bioavailability for the microorganisms [4,12].

In the past decades, new strategies to increase the mass transfer of hydrophobic VOCs have been developed. Among them, the addition of surfactants has shown to be promising [11,12]. Surfactants are amphiphilic compounds (containing both hydrophobic and hydrophilic parts) that decrease the surface and interfacial tension between two immiscible phases (e.g. liquid-gas, liquid-liquid and/or solid-liquid) and significantly increase the solubility of a compound in a medium [12,13]. The increase in solubility is attributed to the formation of micelles, an aggregate of surfactant molecules where the hydrophilic heads of the surfactant monomers are at the outer periphery to maximize their contact with water, while the hydrophobic tails are in the center forming a hydrophobic entity with a preference to sparingly soluble compounds. Generally, these micelles are formed when a surfactant is added beyond the Critical Micelle Concentration (CMC) [14]. For example, Mokhtari et al. [15] have indicated that the removal of n-hexane in biofilters can be enhanced with the addition of rhamnolipid (CMC: 10-200 mg L^{-1}), a biological surfactant. The results indicated that in the presence of the biosurfactant at 300 mg L^{-1}, the removal efficiency (RE) of n-hexane at an inlet load (IL) of 8.4-29.3 g m^{-3} h^{-1} and an empty bed residence time (EBRT) of 120 s increased from 47 ± 8% to 85 ± 10%. Similarly, Aly Hassan & Sorial [16] reported an increase in the RE (from 57 to 68%) of n-hexane in a biotrickling filter when Tomadol 25-7 was used at 1 CMC (150 mg L^{-1}). The biotrickling filter was operated at an IL of 10.4 g m^{-3} h^{-1} and an EBRT of 120 s. In both cases, the authors concluded that the performance improvement was due to an increase in n-hexane solubility and thus, an increase in the bioavailability of the VOC for the microorganisms. As confirmed experimentally by Wu et al. [17], the increased bioavailability of hydrophobic VOCs can have positive effects on the hydrophobicity of microorganisms and promote the succession and activity of specialized microbial communities that will ultimately improve the performance of a bioreactor.

It is well known that for instance in biofilters, the performance correlates with the dimensionless gas-liquid equilibrium partitioning coefficient (K_{GL}) of the compounds (Eq. 1). Literature indicates that the lower the K_{GL} value of a compound (i.e. a higher affinity for the liquid phase), the more bioavailable and easier it is to remove it [11].

$$K_{GL} = \frac{C_{gas}}{C_{liquid}}\ (-) \qquad \text{Eq. 1}$$

Therefore, to gain an understanding and expand the applicability of surfactants in biological gas treatment techniques, the effect of surfactant type and concentration on the K_{GL} (i.e. increase of solubility) of hydrophobic VOCs is paramount. So far, limited research has been carried out on this. Except for one study about n-hexane [18], the determination of K_{GL} coefficients has been focused on compounds in the low range of K_{GL}(-) (< 5) and only with surfactants of synthetic origin. For example, Vane & Giroux [19] studied the influence of the anionic surfactant sodium dodecyl sulfate (SDS; CMC = 2360 mg L^{-1}) on the K_{GL} of toluene at 30 °C and found a decrease in K_{GL} of 84% when a concentration up to 20 000 mg L^{-1} was added. Anderson [13] added SDS (CMC = 865 mg L^{-1} in 0.03 M NaCl) at 8652 mg L^{-1} to a solution of toluene in water at 23 °C, resulting in a significant K_{GL} decrease up to 53%. Contrary, the influence of low concentrations (sub-CMC) of SDS (28.8 – 865 mg L^{-1}) resulted in negligible decreases (0 – 6%) [13]. According to Vane & Giroux [19], hydrophobic zones of the surfactants to which VOCs partition are only created when micelles are formed, and concentrations below the CMC (i.e. sub-CMC quantities) should not alter the K_{GL} values since no separate hydrophobic zones are available. Valsaraj et al. [20], Helburn et al. [21], and Shimotori & Arnold [22] among others have concluded that the partitioning coefficients are unaffected and/or not statistically different from those in pure water until the surfactant concentrations are around the CMC. This was corroborated with experiments for chloromethanes in water containing SDS, sodium dodecylbenzene sulfonate (SDBS), and hexadecyl trimethyl ammonium bromide (HTAB); for limonene, β-pinene, TCE and toluene in water containing SDBS, tetradecylbenzyl dimethyl ammonium chloride (TDBAC) and a linear alkyl ethoxylate mixture (Neodol 1.9); and for chlorinated ethylenes in water containing Triton X-100, SDS, and CTAB, respectively. This indicates that the interactions between the surfactant and the target compound are negligible at concentrations below the CMC.

This study evaluates the effect of 2 synthetic surfactants, i.e. SDS (anionic) and Tween 80 (nonionic), and 3 biological surfactants, i.e. surfactin, rhamnolipid and saponin, at different concentrations (0, 1 and 3 CMC) on the K_{GL} of 7 hydrophobic VOCs, i.e. toluene, ethylbenzene, m-xylene, cyclohexane, pentane, hexane and heptane. The synthetic surfactants were selected as model compounds given their bulk and commercial availability, their difference in charge of the head groups, and their previous application in biofiltration systems [23–25]. The biological surfactants were selected because they are known to be less toxic and more environmentally friendly [26]. Since the final goal is to use the (bio)surfactants as a strategy to enhance the removal of hydrophobic VOCs in gas-phase bioreactors, cationic surfactants were not included as they are well known to be toxic for microorganisms [27,28]. The 7 VOCs were selected over a broad range of low water solubilities (Table S2), and due to their relevance at the industrial level. For example, these VOCs are commonly emitted by petrochemical industries and/or are present in residual gases from the production of solvents, paints and polymers, among others [29,30]. Moreover, due to the broad range of K_{GL} coefficients, two measuring methodologies, i.e. the Dynamic Absorption method (DynAb) and the equilibrium partitioning in close system method (EPICS) were evaluated and optimized in this study. The DynAb is based on the absorption of VOCs in a liquid volume from a constant gas concentration. The monitoring of the outlet gas concentration results in a compound concentration profile (i.e. breakthrough curve) that is used to calculate the K_{GL} [31]. Contrary, in the EPICS method the K_{GL} is obtained by measuring the gas headspace concentration ratios from paired sealed bottles containing different volumes of liquid under equilibrium conditions [32]. To the best of our knowledge, this is the first study where the effect of biological surfactants on the K_{GL} is evaluated, and so far, there are only very few experimentally determined K_{GL} values for the (cyclo)alkanes. This paper provides fundamental data for future studies that aim to enhance the mass transfer of hydrophobic VOCs in bioreactors. Moreover, the determined K_{GL} values can be used to improve the design and modeling of air treatment systems where surfactants are used.

2. Materials and methods

2.1 Experimental reagents

All chemicals described below were used without further purification. For the DynAb method, a certified gas cylinder (NIPPON GASES, Oevel, Belgium) containing toluene, m-xylene, ethylbenzene, cyclohexane, pentane, hexane and heptane in N_2 was used. Each VOC was present at 50 ppm_v. For the EPICS method, the following reagents were used: methanol (assay: 99.9+% Merck, Darmstadt, Germany), cyclohexane (assay: 99.9% Merck, Darmstadt, Germany), pentane (assay: 99.5% Sigma-Aldrich, Bornem, Belgium), hexane (assay: 97+% Fisher Scientific, Merelbeke, Belgium) and heptane (assay: 99+% Sigma-Aldrich, Bornem, Belgium).

To determine the influence of type and concentration of (bio)surfactant on the K_{GL} in both experimental set-ups, two synthetic surfactants, i.e. Tween 80 (assay: not reported; Sigma-Aldrich, Bornem, Belgium) and SDS (assay: ≥ 98.5%; Sigma-Aldrich, Bornem, Belgium), and three biosurfactants, i.e. surfactin (assay: > 90%; Kaneka Corporation, Tokyo, Japan), rhamnolipid (assay: 90%; AGAE technologies, Oregon, United States) and saponin (Saponin Quillaja sp. - Sapogenin content: 20 - 35%; Sigma-Aldrich, Bornem, Belgium), were selected (Table S3). The experiments were carried out at 0 (no surfactant), 1 and 3 CMC. Additionally, 1 mL of an antifoam (XIAMETER AFE-0110 (Dow, Terneuzen, Netherlands)) dilute solution (1:10 v/v in water) was added in all experiments to avoid foam formation that could affect the analytical instruments. The inference of the antifoam solution with the measurements was checked (see section 2.2).

2.2 DynAb method

In the Dynamic Absorption method (DynAb method), a gas stream with a known and constant concentration of VOCs is bubbled through a known liquid volume (in this case, water, or water + surfactant). Hereby, the VOCs are transferred from the gas phase into the liquid phase until equilibrium is reached. The outlet gas concentration is continuously measured, which results in a compound concentration profile (i.e. breakthrough curve) that is used to calculate the partitioning coefficient [31].

A schematic overview of the set-up used in this study is given in Fig. 1 and a detailed description of the construction and working process can be found in the supplementary material (Text S1). Briefly, two main gas streams were used for each experiment. One containing the individual target VOCs in N_2, and further diluted with N_2, and an additional N_2 stream used to flush the lines and bubble column before starting. The bubble column contained the known volume of liquid and was temperature-controlled (25 °C) in a thermostatic cabinet. The absorption of VOCs in the liquid was quantified by continuously measuring the outlet gas stream of the bubble column until equilibrium with the gas phase was reached (i.e. the VOC concentration at the outlet was equal to the concentration at the inlet). For this, Selected Ion Flow Tube Mass Spectrometry (SIFT-MS) was used. SIFT-MS is a technique based on the chemical ionization of pollutants using precursor ions such as NO^+, H_3O^+ and O_2^+ (Voice 200, Syft technologies, Interscience, Louvain-La-Neuve, Belgium). The product ions (and their precursor ions) for this study were selected based on (i) their branching ratio (BR – relative abundance = 100 %), (ii) reaction rate (≥ $1.7x10^{-9}$ molecules cm^{-3} s^{-1}), (iii) signal stability (Relative Standard Deviation (RSD) < 10%), and (iv) interference between compounds. In this way, $C_7H_8^+$ [92]/NO^+ was selected for toluene, $C_8H_{10}^+$ [106]/NO^+ for ethylbenzene, $C_8H_{10}^+$ [106]/NO^+ for m-xylene, $C_6H_{11}^+$ [83]/H_3O^+ for cyclohexane, $C_5H_{12}^+$ [72]/O_2^+ for pentane, $C_6H_{13}^+$ [85]/NO^+ for hexane, and $C_7H_{15}^+$ [99]/NO^+ for heptane. Since all the product ions of ethylbenzene and m-xylene overlap (same mass-to-charge (m/z) ratio), the results are shown as ethylbenzene + m-xylene (as a mixture) in the following sections.

The absorption of the compounds in the liquid results in a breakthrough curve similar to Fig. 2 (grey curve), while the black curve represents the blank correction (i.e. no liquid present, see Text S1). The area (A) between both curves is proportional to the mass of VOCs absorbed in the liquid phase [31]. The time needed to reach equilibrium (~80 min. in Fig. 2) depends among other factors on e.g. the affinity of the VOC to the liquid phase and the volume of liquid. As such, for VOCs that are more soluble in water or water + surfactant, it takes longer to reach equilibrium, and the larger the volume of liquid, the longer the measurement time. For details in the calculation of the K_{GLs}, the reader is referred to the supplementary material (Text S2).

All experiments were carried out in triplicate and, when performing the experiments with (bio)surfactants, 1 mL of XIAMETER AFE-0110 antifoam solution (1:10 v/v dilution in water) was added to avoid foam formation that could disturb the SIFT-MS measurements. The influence of antifoam on the K_{GL} measurements was investigated and no statistically significant difference was found between adding antifoam or not (e.g. K_{GL} of toluene + 2.5 mL antifoam = 0.36 ± 0.01 versus K_{GL} of toluene without antifoam = 0.33 ± 0.03).

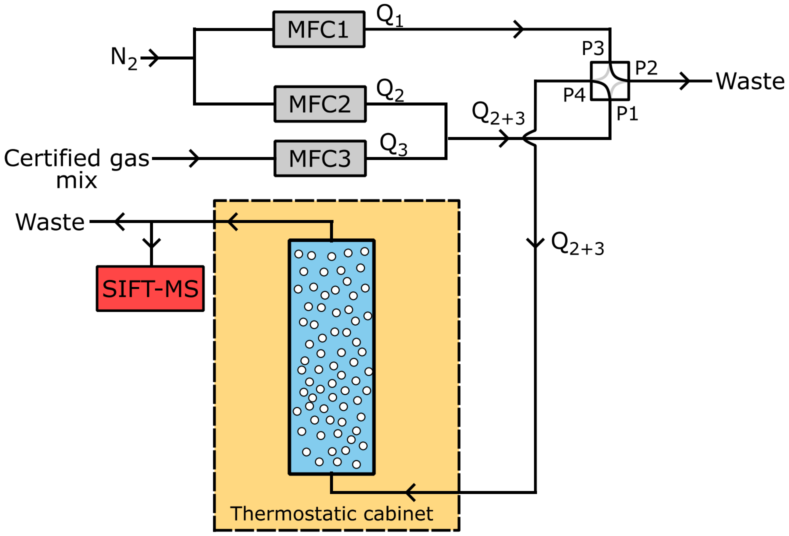

Figure 1. Schematic overview of the experimental set-up of the DynAb method. MFC stands for Mass Flow Controller and SIFT-MS for Selected Ion Flow Tube Mass Spectrometry.

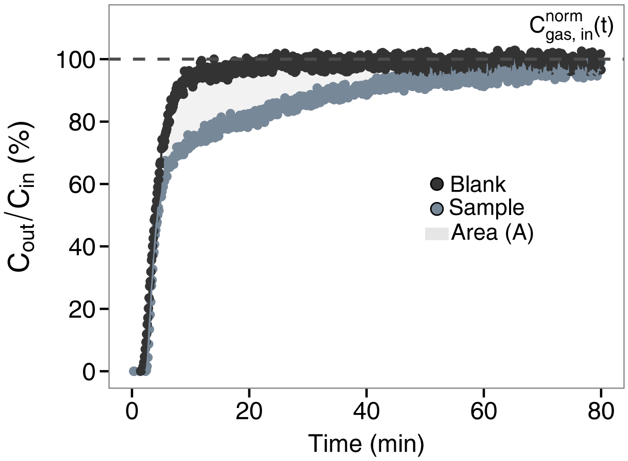

Figure 2. Breakthrough curves of the normalized gas phase concentration (C_{out}/C_{in}) as a function of time (min) in a bubble column without liquid (blank correction - black dots) and with liquid (grey dots). The grey area (A) between both curves is proportional to the mass of the compounds absorbed in the liquid phase.

2.3 EPICS method

The EPICS method consists of sealed two-phase (gas-liquid) batch systems with different volumes of liquid and under equilibrium conditions. The gas-phase concentration of paired systems is measured and the dimensionless K_{GL} is calculated based on mass balance equations (Gossett, 1987).

In this study, 8 bottles of 119.3 ± 0.4 mL were selected. Three (3) contained 5 ± 0.01 mL of liquid (water or water + surfactant) while the other 5 bottles contained 115 ± 0.01 mL of liquid. The liquid volumes were determined based on the modeling approach explained in the supplementary material (Text S3). Moreover, 5 bottles (instead of 3) were employed for the big volumes of liquid (115 mL) for practical reasons. The headspace volume in the latter case is only 4 mL and the extraction of a gas sample required careful handling.

Twenty (20) µL of a stock solution containing cyclohexane, pentane and hexane, was injected under the water surface of each bottle using a 25 µL syringe (Vici, Louisiana, USA). The syringe was weighed before and after injection to obtain a gravimetric precision of 0.0001 g. After injection, the vial was immediately closed with a Mininert valve (BGB Analytik, Harderwijk, The Netherlands). The bottles were placed overnight in a water bath at 25 °C and shaken at 100 rotations per minute (rpm) to allow equilibrium. Finally, 100 µL was carefully taken from the headspace (100 µL syringe Pressure-Lok Series, Vici, Louisiana, USA) and injected into a gas chromatograph (GC) (see Text S4).

The combination of all bottles with different volumes of liquid resulted, in most cases, in 15 estimations of K_{GL} coefficients. As mentioned in section 2.2, when performing the experiments with (bio)surfactants, 1 mL of XIAME AFE-0110 antifoam solution (1:10 v/v dilution in water) was also added to avoid foam formation which in this case could disturb the GC measurements.

2.4 Data analysis

Mean values with standard deviations (SD) were calculated for all the K_{GL} measurements, i.e. for each target compound and (bio)surfactant concentration. To determine if there were significant differences between measurements, a one-way Analysis of Variance (ANOVA) was performed for each compound and concentration of (bio)surfactant (0, 1, and 3 CMC). In this case, the respective assumptions (i.e. equality of variances (Levene's Test) and normality (Shapiro-Wilk test)) were verified, followed by a post hoc analysis. The Tukey's Honest Significant Difference Method was used, but in cases where the assumption of normality was not met, the non-parametric "Kruskal-Wallis ranksum test" was used, followed by the Wilcoxon rank-sum test for the pairwise comparisons. In all analyses, the statistical significance was reported at the 95 % confidence level (*P* ≤ 0.05). All analyses were conducted in RStudio version 4.0.2 (RStudio Team, 2020).

3. Results and discussions

3.1 Applicability assessment and optimization of the DynAb and EPICS methodology to measure K_{GL} of hydrophobic VOCs

Preliminary measurements were carried out to check the applicability of both methods (DynAb and EPICS) for all selected VOCs. First, 2 volumes (100 mL and 2500 mL) of water were used for the DynAb method following the methodology explained in section 2.2. From this, no statistical difference was observed between both volumes for the K_{GL} coefficients of m-xylene + ethylbenzene and toluene (Table 1). Nevertheless, a volume of 100 mL was too small to observe the absorption of pentane, hexane and heptane in water, and a volume of 2500 mL was still not enough to achieve reproducible and accurate (based on literature) coefficients. According to Bruneel et al. [31] a sufficiently large area between both curves (absorption and blank correction breakthrough curve) is required in the DynAb method because small variations of the determined area (e.g. due to instrumental variability) lead to high imprecision in the K_{GL} values. This area could be enlarged by, for example, increasing the volume of liquid. However, the time necessary to determine the K_{GL} coefficients is dependent on the liquid volume and, for compounds with low K_{GL} values, this results in a longer measurement time. Therefore, a balance must be achieved to obtain accurate and reproducible K_{GL} values within reasonable measurement times. From this preliminary experiment, a volume larger than 2500 mL would be needed for the most hydrophobic VOCs, which would lead to measuring times of more than 12 h for the less hydrophobic ones (i.e. toluene and m-xylene + ethylbenzene). Moreover, since the addition of surfactants lowers the K_{GL} coefficient, the measuring time would be even larger, especially for the less hydrophobic VOCs.

Table 1. Average K_{GL} ± standard deviation (SD) and corresponding relative standard deviation (RSD, %) for all VOCs in the two volumes of water tested in the DynAb method. All measurements were carried out in triplicate.

Compound	**V=2500 mL**		**V=100 mL**	
	K_{GL} ± SD	**RSD (%)**	**K_{GL} ± SD**	**RSD (%)**
m-Xylene + Ethylbenzene	0.38 ± 0.05	12	0.39 ± 0.10	26
Toluene	0.35 ± 0.03	9.9	0.33 ± 0.03	8.8
Pentane	7 ± 91	1313	-	-
Hexane	9.3 ± 4.8	51	-	-
Heptane	5.0 ± 1.9	38	-	-

K_{GL} values for pentane, hexane and heptane with 100 mL are not shown (-) because no absorption of VOCs in the water was observed. In addition, cyclohexane is not included as the signals available in the Syft library ($C_6H_{13}^+$ [85]/H_3O^+ and $C_6H_{11}^+$ [83]/H_3O^+) were not stable and/or interfered with other compounds.

On the other hand, the EPICS method relies on the difference in liquid volume between two bottles. The technique has its maximum sensitivity the greater the differences between the two volumes [33,34]. The volume required to have less variability between measurements can be estimated by considering the variables that contribute the most to the measurement (see supplementary material, Text S3). However, as reported by Dewulf et al. [33] and observed in this study, the variability (expressed as RSD, %) increases exponentially with decreasing K_{GL} and, in practice, this variability can be up to 4 times higher than the predicted one. Therefore, the determination of K_{GL} coefficients for toluene, m-xylene and ethylbenzene and their decrease in the presence of surfactants and the conditions used in this study, would lead to high uncertainty.

These preliminary experiments and considerations clearly show that, because of the broad range of K_{GL} coefficients, the use of one single method is not possible for the entire set of compounds and (bio)surfactants. Therefore, the K_{GL} coefficients of the most water-soluble compounds (i.e. toluene and m-xylene + ethylbenzene) were determined with the DynAb method, while the K_{GL} coefficients of the most hydrophobic compounds (i.e. cyclohexane, pentane, hexane and heptane) were measured with the EPICS method.

In both cases, the methods were optimized for each set of compounds. For the DynAb method, a minimum sufficient liquid volume (water or water + surfactant: 100 mL) that leads to reproducible K_{GL} values and within reasonable measurement times (maximum 4 hours, depending on the experiment) was selected. For the EPICS method, theoretical modeling was performed (see supplementary material, Text S3) to determine the volume of liquid needed in each bottle to improve the precision of the method in the desired range of K_{GL} values. The result is shown in Figure 3. Optimal conditions were found when V_{w1} and V_{w2} are respectively 5 mL and 115 mL, which is the largest difference in volumes between paired bottles. This has been corroborated by Dewulf et al. [33], who concluded that the larger the difference in volumes between paired bottles, the smaller the RSD on the K_{GL}. From Figure 3A and B, a sharp increase in RSD is present when K_{GL} values below 0.1 are measured for any combination of liquid volumes. For higher K_{GL} coefficients (> 0.5), the increase in RSD changes substantially depending on the combination. The RSD of the experimentally determined K_{GL} values for cyclohexane, pentane, hexane and heptane in water is depicted in Figure 4. In general, the trend predicted by the model is followed by the experimental results.

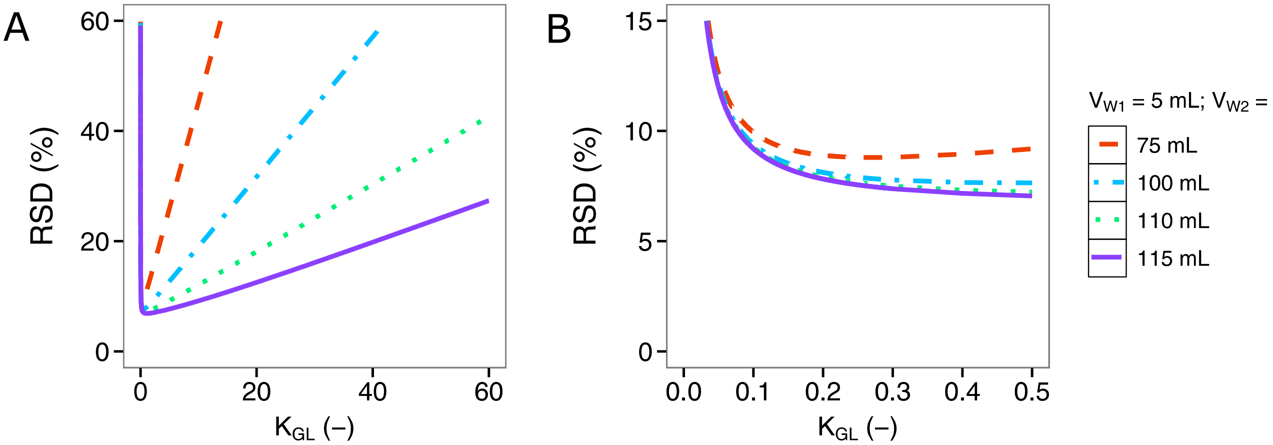

Figure 3. Expected relative standard deviation (RSD) (%) of K_{GL} (-) determined with the EPICS method as a function of K_{GL} and the volume of liquid in the bottles. The modeling is presented for both A) a larger range of K_{GL} and B) a smaller range of K_{GL}.

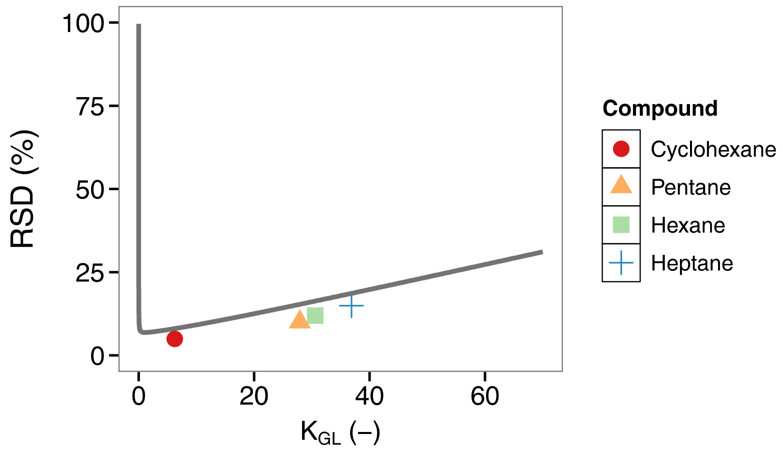

Figure 4. Experimental versus predicted relative standard deviation (RSD) (%) on K_{GL} (-) when using the EPICS method with V_{w1} = 5 mL and V_{w2} = 115 mL, and water as the liquid phase. The gray line graph represents the theoretical modeling, while the data points show the experimentally determined values.

3.2 Experimentally determined K_{GL} coefficients

The experimentally determined K_{GL} coefficients for the compounds of interest are shown in Table 2, and the trend of the effect of surfactant concentration as well as the percentage of the decrease in K_{GL} is depicted in Figure 5. The decrease in K_{GL} is calculated relative to the K_{GL} when no (bio)surfactant was present (i.e. 0 CMC). Moreover, the dotted line shown in Figure 5 does not represent continuous values of K_{GL} for the number of CMC (#CMC) but merely connects the measured points at 0, 1 and 3 CMC to guide the eye.

3.2.1 Partitioning of VOCs between gas and water

The lowest partitioning coefficient was obtained for toluene (0.33 ± 0.03), followed by m-xylene + ethylbenzene, while the highest was for heptane (36.9 ± 5.5). In fact, the increase in partitioning follows the decrease in water solubility presented in Table S2 for each VOC, i.e. toluene < ethylbenzene + m-xylene < cyclohexane < pentane < hexane < heptane.

Partitioning of toluene, m-xylene and ethylbenzene between air and water has been extensively investigated, and a broad range of K_{GL} values at 25 °C have been experimentally determined. As such, according to a comprehensive summary of K_{GL} coefficients made by Sander [35], authors such as Peng & Wan [36], Falabella & Teja [37], Lau et al. [38], Park et al. [39], Schoene & Steinhanses [40], and Hoff et al. [41] have reported experimental K_{GL} values for toluene (range: 0.31 – 0.34) in the same order of magnitude as the one measured in this study. Similarly, authors such as Kim & Kim [42], Jianjun & Carr [43] and Ashworth et al. [44] have reported a K_{GL} value of 0.31 for m-xylene, whereas for ethylbenzene, Lodge & Danso [45], Ryu & Park [46], Turner et al. [47] and Bissonette et al. [48] have reported a K_{GL} of 0.37. Even though the analytical technique used (SIFT-MS) did not allow us to distinguish between m-xylene and ethylbenzene, the obtained K_{GL} for the mixture of both compounds is in the same order of magnitude as the K_{GL} values reported in literature for each compound. Contrarily, the K_{GL} coefficients for cyclohexane, pentane, hexane and heptane in an air-water system are only rarely experimentally determined. For cyclohexane, Ashworth et al. [44], Helburn et al. [21] and Dewulf et al. [49] have obtained K_{GL} values at 25 °C between 5.07 – 7.33, which is in the same order of magnitude as the K_{GL} coefficient determined in this study. According to the compilation of Sander [35], a larger range of K_{GL} coefficients is observed for pentane, hexane and heptane, with differences in K_{GL} values by a factor of up to 2.7 times per compound.

For both hexane and heptane, respectively, Ashworth et al. (1988) (K_{GL} = 31.4) and Hansen et al. (1993) (K_{GL} = 33.6) determined a K_{GL} coefficient close to the K_{GL} determined in this study. Whereas for pentane, the only 3 experimental determined K_{GL} values available are larger (37 – 57) [50–52] than the value obtained in this study. However, these values were obtained by techniques other than the EPICS method used in this case.

3.2.2 Partitioning of VOCs between gas and (water + surfactant)

The addition of (bio)surfactants at concentrations higher than or equal to its CMC results in all cases in a decrease in the K_{GL} coefficient by 5 to 96%, depending on the compound and surfactant of interest. The smallest decrease is observed for pentane when surfactin was added at 1 CMC, while the most pronounced decrease is obtained for heptane when SDS was added at 3 CMC. For m-xylene + ethylbenzene, toluene and heptane, a larger decrease is observed between adding no (bio)surfactant and adding (bio)surfactant at a concentration equal to 1 CMC, than between adding 1 CMC and 3 CMC. Contrary, for cyclohexane, pentane and hexane, an increase in concentration from 1 CMC to 3 CMC of SDS, surfactin and rhamnolipid decreased the K_{GL} coefficients up to 3.7 times. In all cases, no statistically significant difference ($P > 0.05$) is observed when Tween 80 was added at 1 or 3 CMC. In general, rhamnolipid and SDS performed better than other (bio)surfactants in decreasing the K_{GL} coefficient of m-xylene + ethylbenzene and toluene at both concentrations. For cyclohexane, pentane, hexane and heptane, the strongest decreases are observed for SDS followed by saponin, whereas the smallest effect on K_{GL} is observed when Tween 80 and/or surfactin were added. Overall, for the linear alkanes, at both 1 and 3 CMC, the K_{GL} decreased most for heptane, followed by hexane and then pentane.

The strong decrease in K_{GL} when SDS is added has been previously observed for some of the VOCs selected in this study. For instance, Vane & Giroux [19] determined the decrease of K_{GL} for toluene when SDS is added at 2 and 4 CMC (CMC = 2360 mg L^{-1}) but at a temperature of 30 °C. The authors found a decrease of respectively 41 and 67%, which is comparable to the 49 and 71% at 1 and 3 CMC (25 °C) obtained in this study. Similarly, Yang et al. [18] reported the effect of SDS on the K_{GL} of n-hexane at 27 °C and at 1 and 2 CMC (CMC = 2360 mg L^{-1}). Decreases of respectively 52 and 81% were obtained and are comparable to those found in this study at 1 (51% decrease) and 3 CMC (88% decrease) at 25 °C. Finally, the small effect on the K_{GL} of hexane when Tween 80 was added has also been observed by Yang et al. [18]. Even though the authors evaluated concentrations of 100 and 200 CMC, the decrease in K_{GL} was only 11 and 33%. To the best of our knowledge, there are no similar studies for m-xylene, ethylbenzene, cyclohexane, pentane and heptane, nor studies evaluating the effect of biological surfactants on the K_{GL}.

Table 2. Average K_{GL} of m-xylene + ethylbenzene, toluene, cyclohexane, pentane, hexane and heptane for five (bio)surfactants (Tween 80, SDS, surfactin, rhamnolipid and saponin) at 0, 1 and 3 CMC and at 25 °C. The same lowercase letters in superscript (a, b, and c) next to the values within one row indicate no significant difference at $P < 0.05$. For m-xylene + ethylbenzene and toluene (DynAb method) n = 3 (see section 2.2); for the other compounds (EPICS method) n = 9 – 15 (see section 2.3).

Compound	**(Bio)surfactant**	**K_{GL} ± SD (-)**		
		0 CMC	**1 CMC**	**3 CMC**
Toluene	Tween 80	0.33 ± 0.03^{a}	0.22 ± 0.07^{a}	0.23 ± 0.02^{a}
	SDS	0.33 ± 0.03^{a}	0.17 ± 0.04^{b}	0.095 ± 0.017^{b}
	Surfactin	0.33 ± 0.03^{a}	0.18 ± 0.03^{b}	0.14 ± 0.03^{b}
	Rhamnolipid	0.33 ± 0.03^{a}	0.17 ± 0.01^{b}	0.084 ± 0.009^{c}
	Saponin	0.33 ± 0.03^{a}	0.18 ± 0.01^{b}	0.18 ± 0.02^{b}
m-Xylene + Ethylbenzene	Tween 80	0.39 ± 0.10^{a}	0.20 ± 0.07^{b}	0.21 ± 0.02^{b}
	SDS	0.39 ± 0.10^{a}	0.11 ± 0.04^{b}	0.051 ± 0.009^{b}
	Surfactin	0.39 ± 0.10^{a}	0.14 ± 0.03^{b}	0.097 ± 0.018^{b}
	Rhamnolipid	0.39 ± 0.10^{a}	0.12 ± 0.005^{b}	0.054 ± 0.006^{b}
	Saponin	0.39 ± 0.10^{a}	0.14 ± 0.005^{b}	0.12 ± 0.02^{b}
Cyclohexane	Tween 80	6.26 ± 0.31^{a}	4.99 ± 0.21^{b}	4.99 ± 0.09^{b}
	SDS	6.26 ± 0.31^{a}	4.38 ± 0.39^{b}	1.31 ± 0.22^{c}
	Surfactin	6.26 ± 0.31^{a}	5.36 ± 0.38^{b}	4.76 ± 0.10^{c}
	Rhamnolipid	6.26 ± 0.31^{a}	4.96 ± 0.23^{b}	4.10 ± 0.20^{c}
	Saponin	6.26 ± 0.31^{a}	4.52 ± 0.20^{b}	3.40 ± 0.09^{c}
Pentane	Tween 80	27.9 ± 2.8^{a}	22.9 ± 1.5^{b}	24.2 ± 0.7^{b}
	SDS	27.9 ± 2.8^{a}	21.5 ± 3.4^{b}	8.08 ± 1.50^{c}
	Surfactin	27.9 ± 2.8^{a}	26.5 ± 3.7^{a}	22.7 ± 1.1^{c}
	Rhamnolipid	27.9 ± 2.8^{a}	25.7 ± 2.9^{b}	20.3 ± 1.7^{c}
	Saponin	27.9 ± 2.8^{a}	20.9 ± 1.0^{b}	17.0 ± 0.8^{c}
Hexane	Tween 80	30.6 ± 3.7^{a}	18.7 ± 1.1^{b}	19.1 ± 0.1^{b}
	SDS	30.6 ± 3.7^{a}	14.9 ± 1.9^{b}	3.79 ± 0.75^{c}
	Surfactin	30.6 ± 3.7^{a}	24.1 ± 2.9^{b}	21.4 ± 1.0^{c}
	Rhamnolipid	30.6 ± 3.7^{a}	23.1 ± 2.5^{b}	14.5 ± 1.1^{c}
	Saponin	30.6 ± 3.7^{a}	15.8 ± 0.7^{b}	10.1 ± 0.4^{c}
Heptane	Tween 80	36.9 ± 5.5^{a}	12.7 ± 0.7^{b}	12.3 ± 0.3^{b}
	SDS	36.9 ± 5.5^{a}	7.90 ± 0.84^{b}	1.45 ± 0.30^{c}
	Surfactin	36.9 ± 5.5^{a}	19.1 ± 1.9^{b}	17.8 ± 0.9^{b}
	Rhamnolipid	36.9 ± 5.5^{a}	17.0 ± 1.6^{b}	7.92 ± 0.58^{c}
	Saponin	36.9 ± 5.5^{a}	9.12 ± 0.42^{b}	4.52 ± 0.13^{c}

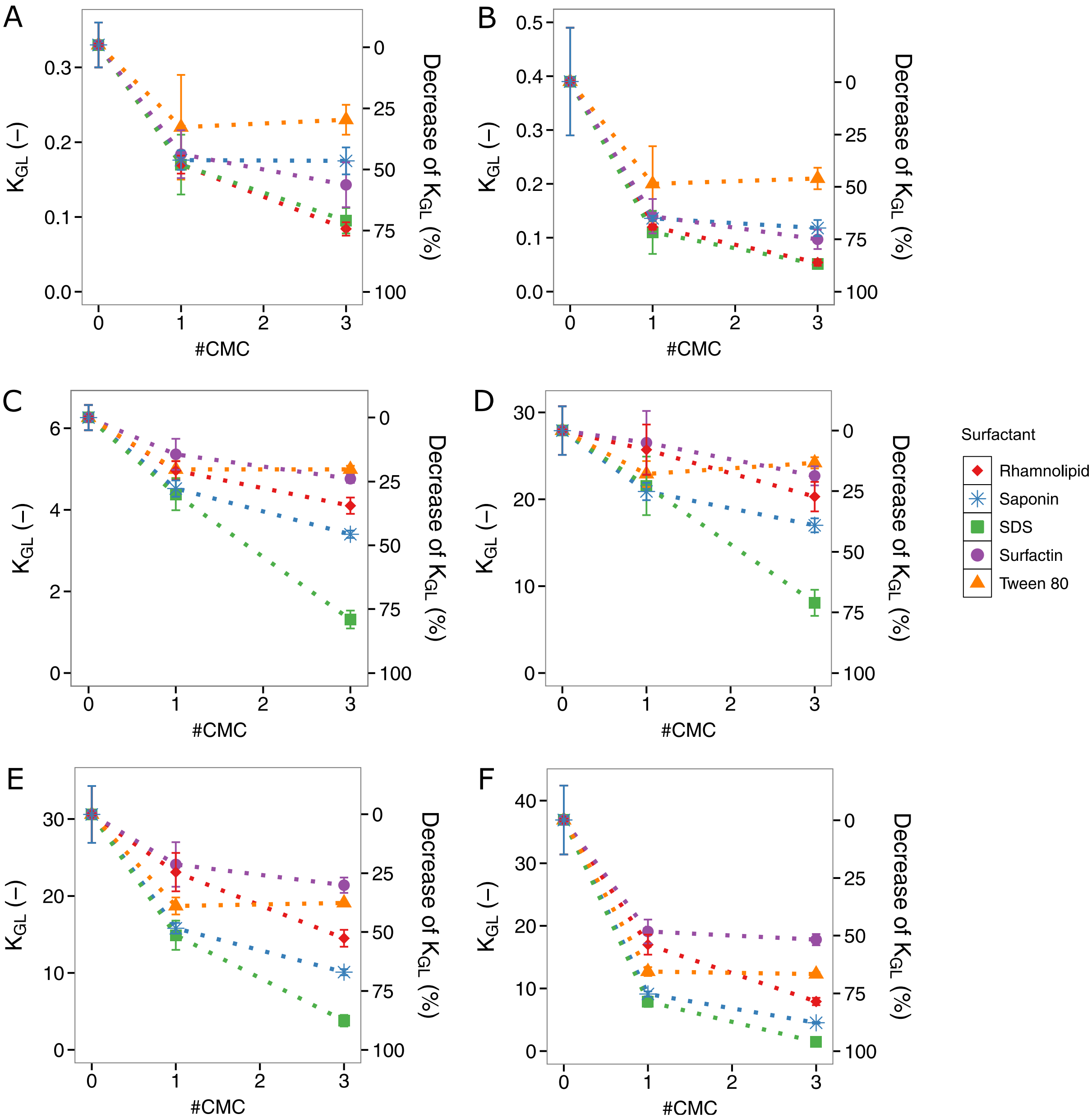

Figure 5. Influence of (bio)surfactants (Tween 80, SDS, surfactin, rhamnolipid and saponin) on the K_{GL} of A) toluene, B) m-xylene + ethylbenzene, C) cyclohexane, D) pentane, E) hexane, and F) heptane: K_{GL} (-) and decrease of K_{GL} (%) as a function of #CMC. The error bars correspond to the standard deviation of the measured K_{GL} values (see section 2.2 & 2.3).

3.2.2.1 Influence of type of (bio)surfactant

One of the most important parameters for (bio)surfactants is the CMC. When the monomer concentration of the (bio)surfactant reaches this CMC, micelles start to form. The driving force for the spontaneous aggregation of (bio)surfactant molecules to form these micelles is hydrophobicity, thus the interior of the micelle consists of the hydrophobic tails. On the contrary, the hydrophilic groups oppose micelle formation. Normally, the charged heads of ionic surfactants often lead to CMC values about 100 times higher than those of non-ionic surfactants [53]. This can be observed when comparing SDS (anionic) and Tween 80 (non-ionic), where the difference is approximately 156 times (see Table S3).

Moreover, depending on the molecular structure, a balance exists between the hydrophilicity and hydrophobicity of the surfactant molecules. This is called the hydrophilic-lipophilic balance (HLB) and it is normally used to categorize surfactants [54]. HLB values were originally developed by Griffin (1954) to classify properties of non-ionic surfactants, ranging from 0 (completely hydrophobic) to 20 (completely hydrophilic). Recently, also ionic surfactants have been assigned relative HLB values, extending the upper limit of the range to 60 [55]. As discussed by Bąk & Podgórska [56], the hydrophobic effect is higher for lower HLB values, which leads to a lower surfactant bulk concentration at which molecules start to aggregate. Consequently, a lower HLB will lead to a lower CMC. A linear relationship between the HLB and the ln(CMC) (mg L^{-1}) (Eq. 2) of the five (bio)surfactants studied here was found (R^2 = 0.95) (Figure 6). This trend has been previously observed by Hait & Moulik [54] for non-ionic surfactants (e.g. for the Tween series (n = 4): ln(CMC) = - 10.49 + 0.88 (HLB); R^2 = 0.98).

$$\ln(CMC) = a + b(HLB) \qquad \textit{Eq. 2}$$

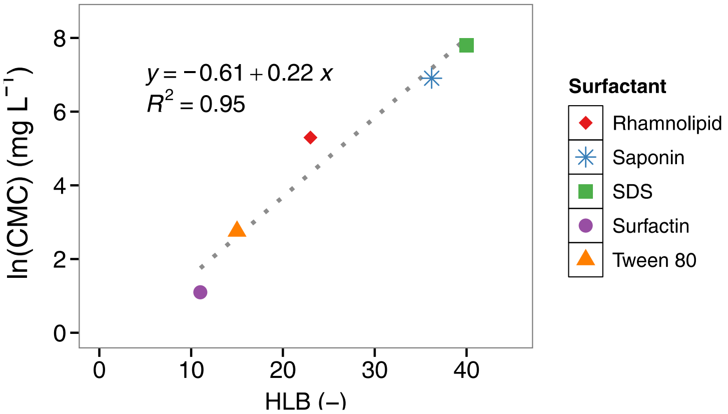

Figure 6. Natural logarithm of the CMC (ln(CMC)) (mg L^{-1}) as function of the hydrophile-lipophile balance (HLB) value (-) for the five (bio)surfactants investigated in this study (see Table S3). Note: average values have been considered when a range of CMC and/or HLB values is present.

As explained in the methodology, the surfactants tested in this study were added on an equal CMC basis and not on a mass basis. Therefore, the (bio)surfactants with a higher CMC were added in larger amounts to the experimental two-phase systems. It could be argued that this larger amount of (bio)surfactant mass influenced the decrease in K_{GL}. In this case, a positive and strong linear ($R^2 \geq 0.7$) relationship was found for the (cyclo)alkanes at 3 CMC between the decrease in K_{GL} and the Log(CMC) when the (bio)surfactants were added (Figure 7). This indicates that the higher the amount of (bio)surfactant added on a mass basis, the stronger the decrease in K_{GL} for these compounds, even if the surfactant addition is the same in terms of CMC. This is reflected in Fig. 5 for the (cyclo)alkanes where SDS (highest CMC, see Table S3) showed the strongest decrease in K_{GL}, while surfactin followed by Tween 80 (lowest CMC) showed the smallest decrease. Similar findings have been reported by Yang et al. [18] and Zhang et al. [57]. In the first study, n-hexane was evaluated in solutions containing SDS (CMC = 2451 mg L^{-1}), cetyltrimethylammonium bromide (CTAB, cationic) (CMC = 335 mg L^{-1}), Triton X-100 (non-ionic) (CMC = 149 mg L^{-1}) and Tween 80 (CMC = 15.7 mg L^{-1}). In the second study, three chlorinated solvents i.e. tetrachloroethylene (PCE), trichloroethylene (TCE) and cis-dichloroethylene (DCE) were tested with SDS (CMC = 2310 mg L^{-1}), SDBS (anionic) (CMC = 520 mg L^{-1}), Triton X-100 (CMC = 110 mg L^{-1}) and Tween 80 (CMC = 15.7 mg L^{-1}). In both cases, the authors concluded that, on a CMC basis, SDS had the greatest effect on the K_{GL} followed by CTAB (in the study of Yang et al. [18]) or SDBS (in the study of Zhang et al. [57]), Triton X-100 and Tween 80. In fact, this order in K_{GL} decrease follows the same sequence of decreasing CMC of all surfactants (i.e. SDS > CTAB or SDBS >

Triton X-100 > Tween 80). However, Zhang et al. [57] concluded that, on a mass basis, the non-ionic surfactants decreased the K_{GL} value more significantly than the anionic surfactants. This was explained by the fact that supra-CMC concentrations were achievable using a lower mass of non-ionic surfactant.

According to Rosen & Kunjappu [58], the solubilization of hydrocarbons can occur at four different sites in the micelle: (i) on the surface of the micelle-solvent interface, (ii) between the hydrophilic head groups, (iii) in the palisade layer, and (iv) in the inner core of the micelle. The authors determined that an increase in monomers (i.e. aggregation number) leads to a higher solubilization capacity for hydrocarbons in the inner core of the micelle. Therefore, (bio)surfactants with a lower CMC such as Tween 80 and surfactin have a smaller solubilization capacity in the inner core of the micelle. As determined in this study and supported by Yang et al. [18] and Zhang et al. [57] for Tween 80, this leads to a weaker decrease in K_{GL}. On the contrary, as SDS has the highest HLB and CMC among the selected (bio)surfactants, it is hypothesized that the larger solubilization capacity for hydrocarbons in the inner core of the micelle can explain the largest decrease of the K_{GL} for all VOCs. In this sense, stronger decreases in K_{GL} can be expected when surfactants with higher HLBs and therefore higher CMCs are employed.

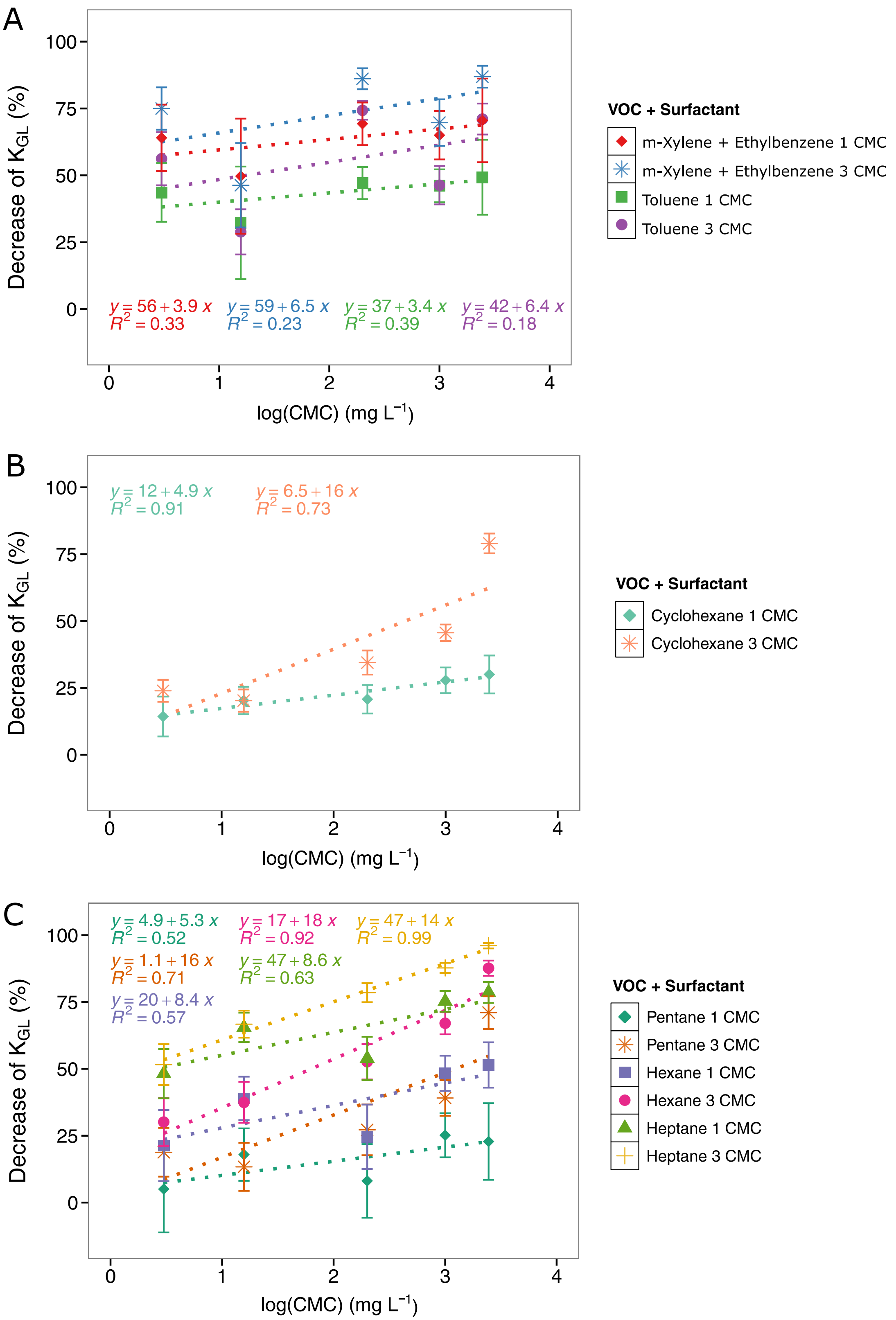

Figure 7. Decrease in the K_{GL} (%) as a function of the Log(CMC) (mg L^{-1}) for A) the aromatic VOCs (m-xylene + ethylbenzene and toluene), B) the cycloalkanes (cyclohexane), and C) the linear alkanes (pentane, hexane, and heptane) when SDS, Tween 80, rhamnolipid, saponin and surfactin are added at respectively 1 and 3 CMC. The error bars correspond to the estimated standard errors associated with the decrease in K_{GL}, calculated according to the law of error propagation.

3.2.2.2 Influence of VOC properties

According to Valsaraj et al. [20], the behavior of hydrophobic halocarbons in micellar media can be described as a pseudo-phase model, in which the micellar phase is considered as a separate, micro-heterogeneous, compartmentalized pseudo-phase that is capable of solubilizing hydrophobic molecules to locally high concentrations. The authors defined the micellar-to-water partitioning coefficient (K_M) and they found a relationship between the K_M and the octanol-water partition coefficient (K_{OW}), indicating that partitioning constants increased with increasing hydrophobicity of the VOCs. In this study, a similar behavior is observed per group of compounds (i.e. aromatic hydrocarbons and (cyclo)alkanes) when the decrease of K_{GL} (%) is plotted as a function of the log(K_{OW}) (see Table S3) for each (bio)surfactant at 1 and 3 CMC (see Figure 8). The trend observed in the decrease of K_{GL} (%) versus the increase in hydrophobicity – especially for the linear hydrocarbons – is in agreement with literature for other compounds such as chloromethanes [20] and chlorinated ethylenes [22]. The reason behind this is the hydrophobic property of the micelle cores. The authors indicate that the more hydrophobic the VOC, the higher its partitioning into the micelles and thus the higher the decrease in its K_{GL}.

Next to hydrophobicity, also polarity plays a role in the partitioning of the VOCs into the micelle phase. Using the dipole moment (D) (see Table S2) as a measure for the polarity of the VOCs, it can be concluded that for the (cyclo)alkanes (D = 0), the differences in the decrease of K_{GL} between them, and hence their partitioning into the micellar phase, can be solely attributed to the differences in their log(K_{OW}) (i.e. hydrophobicity). However, for the aromatics m-xylene + ethylbenzene and toluene, which are polarizable hydrocarbons, their decrease in the K_{GL} can be explained by solubilization (i) in the hydrophobic inner core of the micelle, (ii) at the micelle-water interface (due to polarizability of the π-electron cloud of the aromatic nucleus), and (iii) in the palisade layer [58,59]. Therefore, the solubilization of the aromatics in the different layers is hypothesized as an explanation for the higher decrease of their K_{GL} than would be expected based on solely their log(K_{OW}) [59,60].

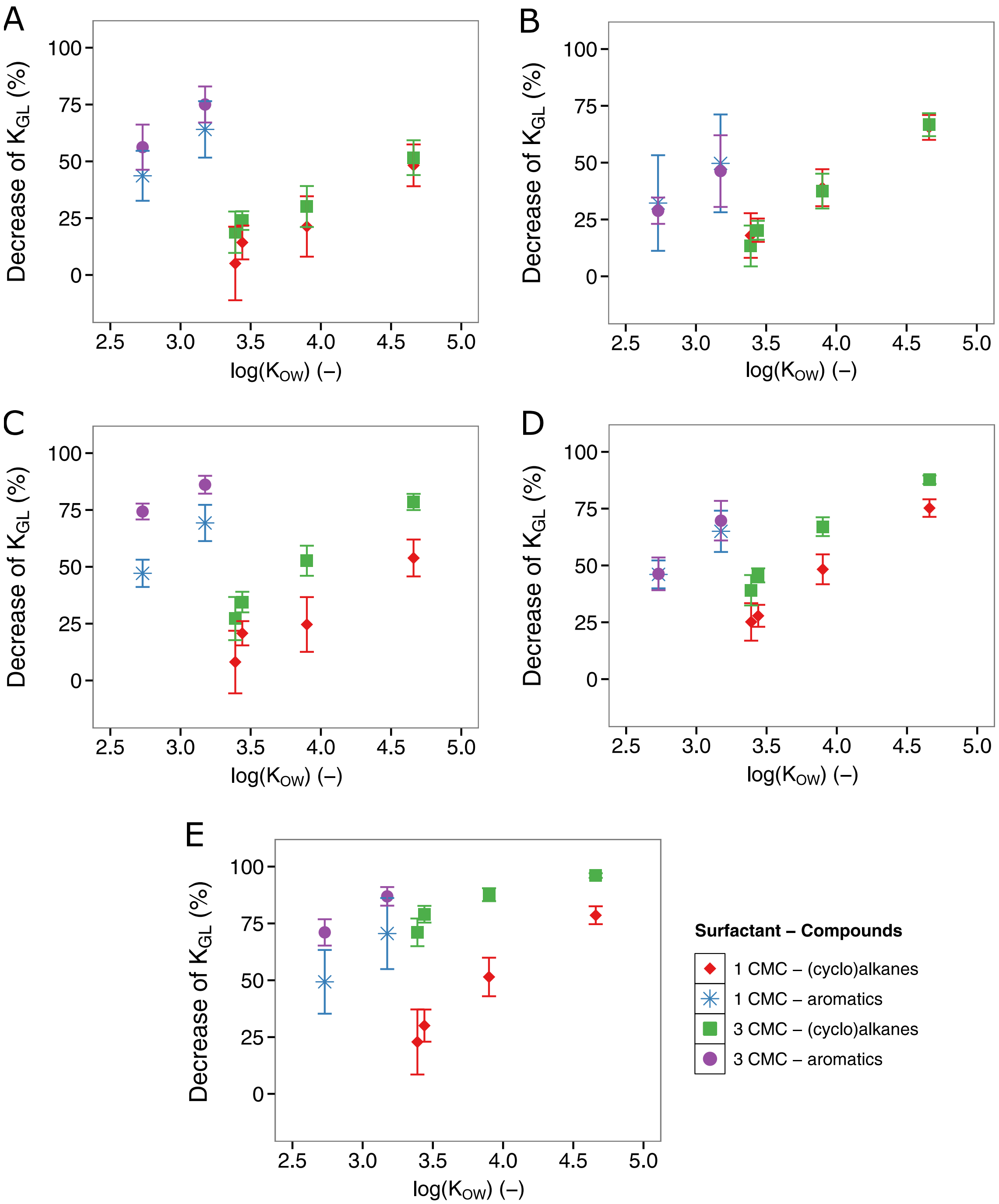

Figure 8. Decrease in the K_{GL} (%) as a function of log(K_{OW}) (-) for the aromatic (m-xylene + ethylbenzene and toluene) and (cyclo)alkane (cyclohexane, pentane, hexane, and heptane) VOCs, when A) surfactin, B) Tween 80, C) rhamnolipid, D) saponin and E) SDS are added at respectively 1 and 3 CMC. The error bars correspond to the estimated standard errors associated with the decrease in K_{GL}, calculated according to the law of error propagation.

4 Conclusions and recommendations

This study provides experimentally determined dimensionless gas-to-liquid partitioning coefficients (K_{GL}) for a broad range of hydrophobic VOCs (toluene, ethylbenzene + m-xylene, cyclohexane, pentane, hexane and heptane) and evaluated the effect of surfactant type (synthetic versus natural and ionic versus non-ionic) and concentration on the K_{GL} of each VOC. Two synthetic surfactants, i.e. SDS and Tween 80, and three biological surfactants, i.e. surfactin, rhamnolipid and saponin, were tested at 0, 1 and 3 CMC. To the best of our knowledge, (i) there are only very few experimentally determined K_{GL} values for the (cyclo)alkanes, and (ii) no study has previously evaluated the effect of biological surfactants on the partitioning between an air and aqueous phase of VOCs.

For all VOCs, a decrease in their K_{GL} of 5 to 96 % was observed when a (bio)surfactant was added at 1 and 3 CMC. For m-xylene + ethylbenzene, toluene and heptane a stronger decrease were observed between the K_{GL} in case no (bio)surfactant was added and when adding (bio)surfactant at a 1 CMC, compared to the difference between adding 1 CMC and 3 CMC. Whereas for cyclohexane, pentane and hexane, an increase in CMC concentration from 1 CMC to 3 CMC of SDS, surfactin, and rhamnolipid led to decreases in K_{GL} coefficients up to 3.7 times. The highest decrease in K_{GL} for all compounds was observed when SDS was added at 3 CMC, and the lowest was when Tween 80 or surfactin was added at both 1 and 3 CMC.

An evaluation of the influence of the (bio)surfactant properties on the decrease in K_{GL} indicates that the HLB value, which represents the relative hydrophobicity of a (bio)surfactant, predominantly determines the decrease in K_{GL} of hydrophobic VOCs. As the driving force for micelle formation is hydrophobicity, it was observed that higher HLB values lead to higher CMCs (i.e. aggregation numbers). A high CMC is thus translated into a higher solubilization capacity for hydrocarbons in the inner core of the micelle, and thus to a larger decrease of K_{GL}. This explains the higher solubilization capacity in the inner core of SDS (having the highest CMC of all selected (bio)surfactants) micelles.

Next to the (bio)surfactant properties, also the log(K_{OW}) and dipole moment of the VOCs showed to influence the decrease in K_{GL}. The (cyclo)alkanes are hypothesized to be solubilized only in the inner core of the micelles, while polarizable hydrocarbons such as m-xylene + ethylbenzene and toluene can be solubilized at the micelle-water interface, in the palisade layer and in the inner core of the micelle.

Overall, this study has shown that all the (bio)surfactants evaluated can improve the solubility of hydrophobic VOCs in water, indicating the potential of (bio)surfactants to improve the removal of hydrophobic VOCs in waste gas treatment technologies. This fundamental data can be used as valuable input to facilitate the selection of a (bio)surfactant and estimate its effect on the performance of different bioreactors. Moreover, the results here obtained can help to improve the design and modeling of air treatment systems where (bio)surfactants are used. K_{GL} coefficients are paramount in modelling approaches. For future studies, the optimal dosage of the (bio)surfactants, their effect on microbial communities, the costs associated with their implementation, and the influence of other parameters (e.g. temperature, pH, dissolved salts, etc.) on the K_{GL} should be further evaluated.

5 Declaration of competing interests

The authors declare that they have no conflict (personal and/or financial) of interest.

6 CRediT authorship contribution statement

Paula Lamprea: Writing-original draft preparation, Data curation, Conceptualization, Methodology, Supervision and Visualization. Max Sabbe: Methodology, Visualization, Data curation. Kristof Demeestere, Herman Van Langenhove, Joren Bruneel and Christophe Walgraeve: Following up and Scientific input, Writing-Reviewing and Editing. Christophe Walgraeve: Conceptualization, Supervision and Resources.

7 Acknowledgments

This work was supported by Ghent University through a special research grant (BOFSTG2019005701) and the authors would like to thank Matis Specialties for supplying a sample of Kaneka Sodium Surfactin.

8 References

[1] European Union, Directive 2010/75/EU of the European Parliament and the Council of 24 November 2010 on industrial emissions (integrated pollution prevention and control), L 334 (2010) 17–119. https://doi.org/10.3000/17252555.L_2010.334.eng.

[2] EPA, PART 59—National volatile organic compound emission standards for consumer and commercila products, Environ. Prot. Agency. (2016) 1–699. https://www.govinfo.gov/content/pkg/CFR-2016-title40-vol6/pdf/CFR-2016-title40-vol6-part59.pdf.

[3] A. Krishnamurthy, B. Adebayo, T. Gelles, A. Rownaghi, F. Rezaei, Abatement of gaseous volatile organic compounds: A process perspective, Catal. Today. 350 (2020) 100–119. https://doi.org/10.1016/j.cattod.2019.05.069.

[4] P. Sarkar, H. Tiwari, P. Garkoti, S. Neogi, J.K. Biswas, A. Dey, Biofiltration as a green technology for abatement of volatile organic compounds (VOCs): A synoptic review, in: M. Shah, S. Rodriguez-Couto, J. Biswas (Eds.), An Innov. Role Biofiltration Wastewater Treat. Plants, Elsevier Inc., 2022: pp. 477–496. https://doi.org/10.1016/b978-0-12-823946-9.00019-x.

[5] C. Kennes, M.C. Veiga, Introduction to air pollution, in: C. Kennes, M.C. Veiga (Eds.), Air Pollut. Prev. Control Bioreact. Bioenergy, John Wiley & Sons, Ltd., Chichester, UK, 2013: pp. 3–18.

[6] F.I. Khan, A.K. Ghoshal, Removal of volatile organic compounds from polluted air, Loss Prev. Process Ind. 13 (2000) 527–545. https://doi.org/https://doi.org/10.1016/S0950-4230(00)00007-3.

[7] T. Kumar, M. Rahul, B. Chandrajit, Biofiltration of volatile organic compounds (VOCs): An overview, Res. J. Chem. Sci. 1 (2011) 83–92.

[8] M.C. Delhoménie, M. Heitz, Biofiltration of air: A review, Crit. Rev. Biotechnol. 25 (2005) 53–72. https://doi.org/10.1080/07388550590935814.

[9] M.M. Amin, A. Rahimi, B. Bina, F. Mohammadi Moghadam, H. Nourmoradi, M. Heidari, Effect of a non-ionic surfactant on xylene removal in a scoria-compost-based biofilter, Clean - Soil, Air, Water. 44 (2016) 1759–1765. https://doi.org/10.1002/clen.201500415.

[10] C. Yang, H. Qian, X. Li, Y. Cheng, H. He, G. Zeng, J. Xi, Simultaneous Removal of Multicomponent VOCs in Biofilters, Trends Biotechnol. 36 (2018) 673–685. https://doi.org/10.1016/j.tibtech.2018.02.004.

[11] P.A. Lamprea Pineda, K. Demeestere, M. Toledo, H. Van Langenhove, C. Walgraeve, Enhanced removal of hydrophobic volatile organic compounds in biofilters and biotrickling filters: A review on the use of surfactants and the addition of hydrophilic compounds, Chemosphere. 279 (2021) 130757. https://doi.org/10.1016/j.chemosphere.2021.130757.

[12] Y. Cheng, H. He, C. Yang, G. Zeng, X. Li, H. Chen, G. Yu, Challenges and solutions for biofiltration of hydrophobic volatile organic compounds, Biotechnol. Adv. 34 (2016) 1091–1102. https://doi.org/10.1016/j.biotechadv.2016.06.007.

[13] M.A. Anderson, Influence of surfactants on vapor-liquid partitioning, Environ. Sci. Technol. 26

(1992) 2186–2191. https://doi.org/10.1021/es00035a017.

[14] C.O. Rangel-Yagui, A. Pessoa-Jr, D. Blankschtein, Two-phase aqueous micellar systems - An alternative method for protein purification, Brazilian J. Chem. Eng. 21 (2004) 531–544. https://doi.org/10.1590/S0104-66322004000400003.

[15] M. Mokhtari, Y. Hajizadeh, A.A. Ebrahimi, M.A. Shahi, N. Jafari, A. Abdolahnejad, Enhanced biodegradation of n-hexane from the air stream using rhamnolipid in a biofilter packed with a mixture of compost, scoria, sugar beet pulp and poplar tree skin, Atmos. Pollut. Res. 10 (2019) 115–122. https://doi.org/10.1016/j.apr.2018.06.008.

[16] A. Aly Hassan, G.A. Sorial, N-hexane biodegradation in trickle bed air biofilters, Water, Air, Soil Pollut. Focus. 8 (2008) 287–296. https://doi.org/10.1007/s11267-007-9149-3.

[17] X. Wu, Y. Lin, Y. Wang, S. Wu, X. Li, C. Yang, Enhanced Removal of Hydrophobic Short-Chain n-Alkanes from Gas Streams in Biotrickling Filters in Presence of Surfactant, Environ. Sci. Technol. 56 (2022) 10349–10360. https://doi.org/10.1021/acs.est.2c02022.

[18] C. Yang, F. Chen, S. Luo, G. Xie, G. Zeng, C. Fan, Effects of surfactants and salt on Henry's constant of n-hexane, J. Hazard. Mater. 175 (2010) 187–192. https://doi.org/10.1016/j.jhazmat.2009.09.147.

[19] L.M. Vane, E.L. Giroux, Henry's law constants and micellar partitioning of volatile organic compounds in surfactant solutions, J. Chem. Eng. Data. 45 (2000) 38–47. https://doi.org/10.1021/je990195u.

[20] K.T. Valsaraj, A. Gupta, L.J. Thibodeaux, D.P. Harrison, Partitioning of chloromethanes between aqueous and surfactant micellar phases, Water Res. 22 (1988) 1173–1183. https://doi.org/10.1016/0043-1354(88)90013-9.

[21] R. Helburn, J. Albritton, G. Howe, L. Michael, D. Franke, Henry's law constants for fragrance and organic solvent compounds in aqueous industrial surfactants, J. Chem. Eng. Data. 53 (2008) 1071–1079. https://doi.org/10.1021/je700418a.

[22] T. Shimotori, W.A. Arnold, Measurement and estimation of Henry's law constants of chlorinated ethylenes in aqueous surfactant solutions, J. Chem. Eng. Data. 48 (2003) 253–261. https://doi.org/10.1021/je025553z.

[23] Y. Hajizadeh, M.M. Amin, K. Ebrahim, I. Parseh, Biodeterioration of 1,1-dimethylhydrazine from air stream using a biofilter packed with compost-scoria-sugarcane bagasse, Atmos. Pollut. Res. 9 (2018) 37–46. https://doi.org/10.1016/j.apr.2017.06.007.

[24] Y. Cheng, H. He, C. Yang, Z. Yan, G. Zeng, H. Qian, Effects of anionic surfactant on n-hexane removal in biofilters, Chemosphere. 150 (2016) 248–253. https://doi.org/10.1016/j.chemosphere.2016.02.027.

[25] Q. Liu, Y.-H. Deng, E.B. Arowolo, Improvement of trickling biofilter purification performance on treating chlorobenzene in waste gases using surfactant, J. Shanghai Univ. 11 (2007) 607–612. https://doi.org/10.1007/s11741-007-0616-1.

[26] C.N. Mulligan, R.N. Yong, B.F. Gibbs, Surfactant-enhanced remediation of contaminated soil: A review, Eng. Geol. 60 (2001) 371–380. https://doi.org/10.1016/S0013-7952(00)00117-4.

[27] J.D. Van Hamme, A. Singh, O.P. Ward, Physiological aspects. Part 1 in a series of papers devoted to surfactants in microbiology and biotechnology, Biotechnol. Adv. 24 (2006) 604–620.

https://doi.org/10.1016/j.biotechadv.2006.08.001.

[28] M.E. Fait, L. Bakas, G.L. Garrote, S.R. Morcelle, M.C.N. Saparrat, Cationic surfactants as antifungal agents, Appl. Microbiol. Biotechnol. 103 (2019) 97–112. https://doi.org/10.1007/s00253-018-9467-6.

[29] H. Cui, Source profile of volatile organic compounds(VOCs) of a petrochemical industry in the Yangtze River Delta,China, Chem. Eng. Trans. 54 (2016) 121–126. https://doi.org/10.3303/CET1654021.

[30] M.M. Amin, A. Rahimi, B. Bina, H. Nourmoradi, M.S. Hassanvand, F. Mohammadi-Moghadam, S. Norouzi, M. Heidari, Biodegradation of n-hexane as single pollutant and in a mixture with BTEX in a scoria/compost-based biofilter, Process Saf. Environ. Prot. 107 (2017) 508–517. https://doi.org/10.1016/j.psep.2017.03.019.

[31] J. Bruneel, C. Walgraeve, K. Van Huffel, H. Van Langenhove, Determination of the gas-to-liquid partitioning coefficients using a new dynamic absorption method (DynAb method), Chem. Eng. J. 283 (2016) 544–552. https://doi.org/10.1016/j.cej.2015.07.053.

[32] J. Staudinger, P. V. Roberts, A critical review of Henry's law constants for environmental applications, Crit. Rev. Environ. Sci. Technol. 26 (1996) 205–297. https://doi.org/10.1080/10643389609388492.

[33] J. Dewulf, D. Drijvers, H. Van Langenhove, Measurement of Henry's law constant as function of temperature and salinity for the low temperature range, Atmos. Environ. 29 (1995) 323–331. https://doi.org/10.1016/1352-2310(94)00256-K.

[34] A.H. Lincoff, J.M. Gossett, The Determination of Henry's Constant for Volatile Organics by Equilibrium Partitioning in Closed Systems, in: W. Brutsaert, G.H. Jirka (Eds.), Gas Transf. Water Surfaces, D. Reidel Publiching Company, 1984: pp. 15–25.

[35] R. Sander, Compilation of Henry's law constants (version 4.0) for water as solvent, Atmos. Chem. Phys. 15 (2015) 4399–4981. https://doi.org/10.5194/acp-15-4399-2015.

[36] J. Peng, A. Wan, Effect of ionic strength on Henry's constants of volatile organic compound, Chemosphere. 36 (1998) 2731–2740.

[37] J.B. Falabella, A.S. Teja, Air-water partitioning of gasoline components in the presence of sodium chloride, Energy and Fuels. 22 (2008) 398–401. https://doi.org/10.1021/ef700513k.

[38] K. Lau, T.N. Rogers, D.J. Chesney, Measuring the aqueous Henry's law constant at elevated temperatures using an extended EPICS technique, J. Chem. Eng. Data. 55 (2010) 5144–5148. https://doi.org/10.1021/je100701w.

[39] S.-J. Park, S.-D. Han, S.-A. Ryu, Measurement of Air/Water Partition Coefficient (Henry's Law Constant) by Using EPICS Method and Their Relationship with Vapor Pressure and Water Solubility, Korean Chem. Eng. Res. 35 (1997) 915–920.

[40] K. Schoene, J. Steinhanses, Determination of Henry's law constant by automated Head space-Gas chromatography - Determination of dissolved gases, Fresenius' Zeitschrift Für Anal. Chemie. 321 (1985) 538–543. https://doi.org/10.1007/BF00464360.

[41] J.T. Hoff, D. Mackay, R. Gillham, W.Y. Shiu, Partitioning of Organic Chemicals at the Air-Water Interface in Environmental Systems, Environ. Sci. Technol. 27 (1993) 2174–2180. https://doi.org/10.1021/es00047a026.

[42] Y.H. Kim, K.H. Kim, Recent advances in thermal desorption-gas chromatography-mass spectrometery method to eliminate the matrix effect between air and water samples: Application to the accurate determination of Henry's law constant, J. Chromatogr. A. 1342 (2014) 78–85. https://doi.org/10.1016/j.chroma.2014.03.040.

[43] L. Jianjun, P.W. Carr, Measurement of Water-Hexadecane Partition Coefficients by Headspace Gas Chromatography and Calculation of Limiting Activity Coefficients in Water, Anal. Chem. 65 (1993) 1443–1450. https://doi.org/10.1021/ac00058a023.

[44] R.A. Ashworth, G.B. Howe, M.E. Mullins, T.N. Rogers, Air-water partitioning coefficients of organics in dilute aqueous solutions, J. Hazard. Mater. 18 (1988) 25–36. https://doi.org/10.1016/0304-3894(88)85057-X.

[45] K.B. Lodge, D. Danso, The measurement of fugacity and the Henry's law constant for volatile organic compounds containing chromophores, Fluid Phase Equilib. 253 (2007) 74–79. https://doi.org/10.1016/j.fluid.2007.01.010.

[46] S.A. Ryu, S.J. Park, A rapid determination method of the air/water partition coefficient and its application, Fluid Phase Equilib. 161 (1999) 295–304. https://doi.org/10.1016/S0378-3812(99)00193-4.

[47] L.H. Turner, Y.C. Chiew, R.C. Ahlert, D.S. Kosson, Measuring vapor-liquid equilibrium for aqueous-organic systems: review and a new technique, Environ. Energy Eng. 42 (1996) 1772–1788.

[48] E.M. Bissonette, J.J. Westrick, J.M. Morand, Determination of Henry's coefficient for volatile organic compounds in dilute aqueous systems, in: Proc. Annu. Conf. Am. Water Work. Assoc., Cincinnati, USA, 1990: pp. 1913–1922.

[49] J. Dewulf, H. Van Langenhove, P. Everaert, Determination of Henry's law coefficients by combination of the equilibrium partitioning in closed systems and solid-phase microextraction techniques, J. Chromatogr. A. 830 (1999) 353–363. https://doi.org/10.1016/S0021-9673(98)00877-2.

[50] F. Jou, A.E. Mather, Vapor - Liquid - Liquid Locus of the System Pentane + Water, J. Chem. Eng. Data. 45 (2000) 728–729.

[51] J.H. Rytting, L.P. Huston, T. Higuchi, Thermodynamic group contributions for hydroxyl, amino, and methylene groups, J. Pharm. Sci. 67 (1978) 615–618.

[52] J.Å. Jönsson, J. Vejrosta, J. Novák, Air/water partition coefficients for normal alkanes (n-pentane to n-nonane), Fluid Phase Equilib. 9 (1982) 279–286. https://doi.org/10.1016/0378-3812(82)80023-X.

[53] A. Helenius, K. Simons, Solubilization of membranes by detergents, Biochim. Biophys. Acta. 415 (1975) 29–79.

[54] S.K. Hait, S.P. Moulik, Determination of Critical Micelle Concentration (CMC) of Nonionic Surfactants by Donor-Acceptor Interaction with Iodine and Correlation of CMC with Hydrophile-Lipophile Balance and Other Parameters of the Surfactants, J. Surfactants Deterg. 4 (2001) 303–309. https://doi.org/10.1007/s11743-001-0184-2.

[55] Merck KGaA, Detergents. A guide to the properties and uses of detergents in biological systems, Darmstadt, Germany, 2017. https://www.sigmaaldrich.com/content/dam/sigma-aldrich/1/content/commerce/pdfs/detergents/detergents-guide-mk.pdf.

[56] A. Bąk, W. Podgórska, Interfacial and surface tensions of toluene/water and air/water systems with nonionic surfactants Tween 20 and Tween 80, Colloids Surfaces A Physicochem. Eng. Asp. 504 (2016) 414–425. https://doi.org/10.1016/j.colsurfa.2016.05.091.

[57] C. Zhang, G. Zheng, C.M. Nichols, Micellar partitioning and its effects on Henry's law constants of chlorinated solvents in anionic and nonionic surfactant solutions, Environ. Sci. Technol. 40 (2006) 208–214. https://doi.org/10.1021/es051387e.

[58] M.J. Rosen, J.T. Kunjappu, Solubilization by Solutions of Surfactants: Micellar Catalysis, Surfactants Interfacial Phenom. (2012) 202–234. https://doi.org/10.1002/9781118228920.ch4.

[59] Z. Cui, J.P. Canselier, Solubilization in some anionic/cationic surfactant binary systems, Polym. Int. 52 (2003) 548–552. https://doi.org/10.1002/pi.1099.

[60] G.A. Smith, S.D. Christian, E.E. Tucker, J.F. Scamehorn, Solubilization of hydrocarbons by surfactant micelles and mixed micelles, J. Colloid Interface Sci. 130 (1989) 254–265. https://doi.org/10.1016/0021-9797(89)90097-0.

Supplementary material:

Text S1. Experimental procedure - DynAb method

A stream (Q_3: 15 mL min^{-1}) was generated from the certified gas mixture containing the individual target VOCs in N_2 and was controlled by a mass flow controller (MFC) (GF Series, Brooks Instruments, USA). Q_3 was further diluted with an N_2 gas stream (Q_2: 30 sccm) to generate the final stream (Q_{2+3}) entering the glass bubble column containing the absorption liquid (i.e. water or water + surfactant). An additional N_2 stream (blank, Q_1: 45 sccm) was installed to flush the lines and the bubble column before starting each experiment. Q_{2+3} and Q_1 were connected to a four-way valve (Swagelok, Belgian fluid system technologies BVBA, Groot-Bijgaarden, Belgium) and, depending on its position, one stream flowed through the column while the other was discarded (waste line). In this way, if the valve was set in “flush mode” (P3 to P4 and P1 to P2) only N_2 flowed through the column, while the diluted stream of VOCs (Q_{2+3}) was vented through the waste line. Contrary, if the valve was set in “compounds mode” (P1 to P4 and P3 to P2), only the diluted stream of VOCs flowed through the column while Q_1 through the waste line. The glass bubble column was equipped with a sintered glass plate (porosity 1: 100 – 160 µm) to enable the generation of small air bubbles. This set-up was temperature-controlled (25 °C) in a thermostatic cabinet (Memmert UM200, Gemini B.V., Apeldoorn, The Netherlands) and all the lines were made of PTFE (polytetrafluoroethylene) tubing.

To start with the measurements, the four-way valve was set in “flush mode” for at least 30 minutes, and at time zero (t_o) the valve was switched to “compounds mode”. In this way, the VOC stream was sent through the bubble column and the compounds were absorbed in the liquid phase until equilibrium with the gas phase was reached (i.e. the VOCs concentration at the outlet was equal to the concentration at the inlet). To account for the possible adsorption of the target VOCs onto the glass column or Teflon tubing, a blank correction was performed. This experiment was carried out with an empty glass bubble column (no liquid added) while keeping all the other parameters constant.

Text S2. Calculation of the partitioning coefficients – DynAb method

The gas-liquid partitioning coefficient (K_{GL}) was determined according to Eq. 1, where C_{liquid}^{norm} is the normalized concentration of VOCs in the liquid phase, V is the liquid volume and Q is the gas flow rate (Q_{2+3}). The normalized gas phase concentration ($C_{gas,sample}^{norm}$ = C_{out}/C_{in}) was calculated as the ratio of the VOC concentration at the outlet and the VOC concentration at the inlet. For practical reasons, it was assumed that equilibrium (t_∞) between the gas and liquid phase was reached when the outlet concentration was equal to the inlet concentration for at least 5 minutes [1].

$$K_{GL} = \frac{C_{gas,in}^{norm}}{C_{liquid}^{norm}} = \frac{1}{\frac{Q\left[\int_{t_0}^{t\infty}\left[1-C_{gas,sample}^{norm}(t)\right]dt-\int_{t_0}^{t\infty}\left[1-C_{gas,blank}^{norm}(t)\right]dt\right]}{V}} = \frac{1}{\frac{Q\,A}{V}} \qquad \text{Eq. 1}$$

Text S3. Calculation of the partitioning coefficients – EPICS method

The following equations, as formulated by Gossett [2], were used for the calculation of the partitioning coefficients. If two bottles (V_b) (1 and 2) are prepared with different liquid volumes V_{L1} and V_{L2} ($V_{L1} < V_{L2}$), the following mass balances can be written:

$$M_1 = C_{g1}\left[(V_{L1}/K_{GL}) + V_{g1}\right] \qquad \textit{Eq. 2}$$

$$M_2 = C_{g2}\left[(V_{L2}/K_{GL}) + V_{g2}\right] \qquad \textit{Eq. 3}$$

where M (g) is the total mass of the compound in the two-phase system, C_g (g mL^{-1}) is the headspace concentration and V_g (mL) is the headspace volume. Solving both equations for K_{GL} results in Eq 4. In this study, r (Eq. 5) was calculated from the ratio of the chromatographic peak areas as the GC detector response was linear in the range of interest.

$$K_{GL} = \frac{V_{L2} - rV_{L1}}{rV_{g1} - V_{g2}} \qquad \textit{Eq. 4}$$

$$r = \frac{C_{g1}/M_1}{C_{g2}/M_2} \qquad \textit{Eq. 5}$$

Finally, to determine the volume of water needed in each bottle (5 mL and 115 mL, section 2.3) and thus improve the precision of the method for the desired range of K_{GL}, theoretical modeling was performed in which the variance (σ^2) of K_{GL} was estimated as a function of K_{GL}. Such a procedure has been carried out before but for compounds with a lower dimensionless K_{GL} coefficient (0.0023 – 13.5) [2-4].

The variance in measured K_{GL} values reflects the variances associated with each of the variables used in its calculation (Eq. 4) [2]. However, this is only valid if the variances on the independent variables are unrelated. In Eq. 4, V_g is dependent on V_L (i.e. $V_g = V_b - V_L$). Thus, rewriting Eq 4. in terms of V_b results in Eq. 6, and the different variance contributions can be written as Eq. 7 and Eq. 8:

$$K_{GL} = \frac{V_{L2} - rV_{L1}}{rV_{g1} - V_{g2}} = \frac{V_{L2} - rV_{L1}}{V_b(r-1) - rV_{L1} + V_{L2}} \quad \text{with } r = \frac{V_b - V_{L2} + V_{L2}/K_{GL}}{V_b - V_{L1} + V_{L1}/K_{GL}} \qquad \textit{Eq. 6}$$

$$\sigma^2(K_{GL}) = \left(\frac{\partial K_{GL}}{\partial V_b}\right)^2 \sigma^2(V_b) + \left(\frac{\partial K_{GL}}{\partial V_{w1}}\right)^2 \sigma^2(V_{L1}) + \left(\frac{\partial K_{GL}}{\partial V_{L2}}\right)^2 \sigma^2(V_{L2}) + \left(\frac{\partial K_{GL}}{\partial r}\right)^2 \sigma^2(r) \qquad \textit{Eq. 7}$$

where:

$$\sigma^2(r) = r^2\left\{\left[\sigma(C_{g1}/M_1)/(C_{g1}/M_1)\right]^2 + \left[\sigma(C_{g2}/M_2)/(C_{g2}/M_2)\right]^2\right\} \qquad \textit{Eq. 8}$$

The variance of each variable was determined experimentally and shown in Table 1 as relative standard deviation (RSD) (i.e. $RSD\ (\%) = 100\ .\ {}^{\sqrt{\sigma^2}}/_{K_{GL}}$).

Table S1. Relative standard deviation (RSD) (%) on factors affecting the variance on the gas-liquid partitioning coefficient (K_{GL}). V_b is the volume of the bottles, V_L is the volume of liquid added, C_g is the headspace concentration, M is the total mass of the compound in the two-phase system, and n is the number of measurements.

Factor	Value	RSD (%)
V_b (mL)	119 (n = 8)	0.31
V_{w1} (mL)	5 [1]	0.20 [1]
V_{w2} (mL)	115 (n = 5)	0.01
C_{g1}/M_1	3.33×10^3 - 3.15×10^4 [2] (n=3)	4.11 – 4.48
C_{g2}/M_2	4.83×10^4 – 4.30×10^5 [2] (n=3)	2.19 – 6.92

[1] Volume was added with a microliter pipette. RSD reported by the supplier [5].

[2] Dependent on the compound added.

Text S4. Experimental procedure – EPICS method

The stock solution contained 5.28 mL cyclohexane, 10.3 mL pentane, 3.13 mL hexane and 1.01 mL heptane in 100 mL methanol and was stored in a fridge at 4 °C. These volumes were calculated in each case so the final water equilibrium concentration was maximally one-tenth of the maximum aqueous solubility [4]. In this way, we ensured that the measurements were conducted in the range where Henry's law (here represented as K_{GL}: gas-liquid partitioning coefficient) is fulfilled (i.e. in dilute solutions) [6].

An Agilent 6890 gas chromatograph (GC) (injector at 220 °C, flame ionization detector (FID) at 250 °C), equipped with a 30 m HP-5 ((5%-phenyl)-methylpolysiloxane) nonpolar column (0.25 µm film thickness, 0.32 mm inner diameter, fused silica capillary tubing) was used to measure the headspace concentration of each bottle. The temperature of the oven was kept constant at 35 °C for 3 min, followed by a temperature rise of 10 °C min^{-1} up to 120 °C. The GC carrier gas was helium at a rate of 6.7 mL min^{-1} and the FID was fed with air at 400 mL min^{-1} and hydrogen at 40 mL min^{-1}.

Table S2. Physical-chemical properties of the VOCs of interest at 25 ˚C. MW stands for molecular weight; WS for water solubility; VP for vapor pressure; K_{OW} for octanol-water partitioning coefficient; and D for debye. Adapted from Howard & Meylan [7] and Dean [8].

Compound	Chemical formula and structure	MW (g mol^{-1})	WS (mg L^{-1})	VP (kPa)	log(K_{OW}) (-)	Dipole moment (D)
Toluene	C_7H_8 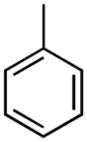	92.1	5.26 x 10^2	3.79	2.73	0.38
m-Xylene	C_8H_{10} 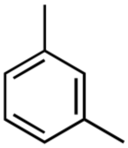	106.2	1.61 x 10^2	1.11	3.20	0.33
Ethylbenzene	C_8H_{10} 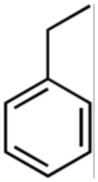	106.2	1.69 x 10^2	1.28	3.15	0.59
Cyclohexane	C_6H_{12} 	84.2	5.50 x 10^1	12.92	3.44	0
Pentane	C_5H_{12} 	72.15	3.80 x 10^1	68.53	3.39	0
Hexane	C_6H_{14} 	86.2	9.50 x 10^0	20.13	3.90	0
Heptane	C_7H_{16} 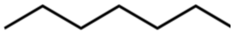	100.2	3.40 x 10^0	6.13	4.66	0

Table S3. (Bio)surfactants and their respective chemical formula, structure, critical micelle concentration (CMC) and hydrophilic-lipophilic balance (HLB). "ni" stands for non-ionic; "a" for anionic, and "n.r" for not reported.

Type of surfactant	Trade name	Average chemical formula and structure	CMC (mg L^{-1})	HLB (-)
Synthetic	Tween 80 (ni)	$C_{64}H_{124}O_{26}$ 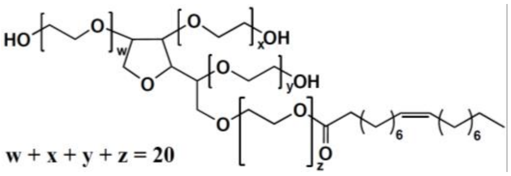	15.72 [1]	15 [1]
	SDS (a)	$C_{12}H_{25}SO_4Na$ 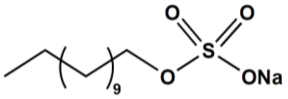	2019 – 2884 [2]	40 [1]
Biological	Surfactin (ni)	$C_{53}H_{93}N_7O_{13}$ 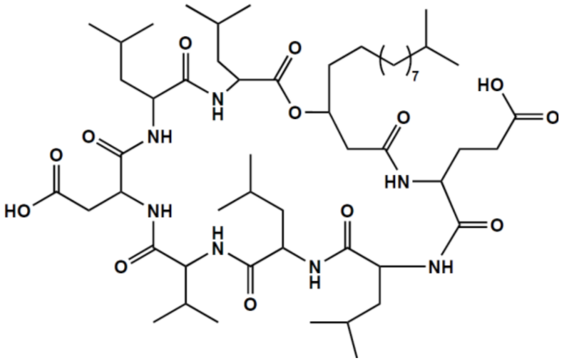	3 [3]	10 – 12 [5]
	Rhamnolipid (ni)	Mono-rhamnolipid dominant: $C_{26}H_{48}O_9$ 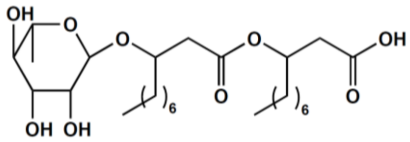 Di-rhamnolipid dominant: $C_{32}H_{58}O_{13}$ 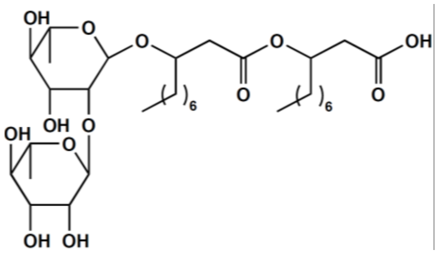	± 200 [4]	22 - 24 [5]
	Saponin (ni)	n.r.	± 1000 [4]	36.3 [6]

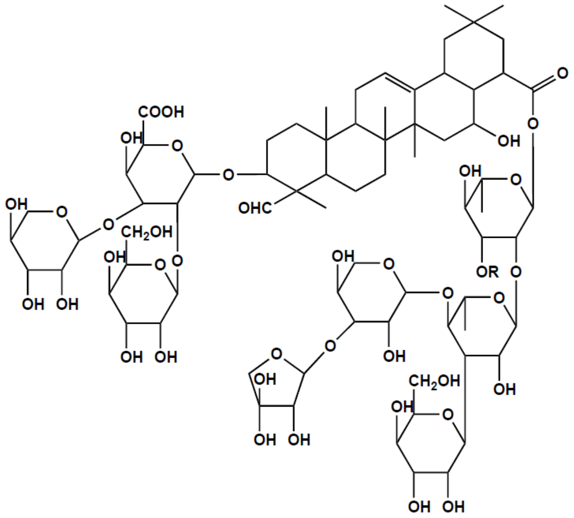

---

[1] [9]

[2] CMC_{avg} = 2451 mg L^{-1} [9]

[3] [10]

[4] [11]

[5] [12]

[6] Value calculated by the authors [13] based on “Davies’ model”, a method developed by Davies [14] to calculate HLB values based on the chemical groups of the molecule with as advantage that it considers the effect of stronger and weaker hydrophilic groups.

References:

[1] J. Bruneel, C. Walgraeve, K. Van Huffel, H. Van Langenhove, Determination of the gas-to-liquid partitioning coefficients using a new dynamic absorption method (DynAb method), Chem. Eng. J. 283 (2016) 544–552. https://doi.org/10.1016/j.cej.2015.07.053.

[2] J.M. Gossett, Measurement of Henry's Law Constants for C1 and C2 Chlorinated Hydrocarbons, Environ. Sci. Technol. 21 (1987) 202–208. https://doi.org/10.1021/es00156a012.

[3] J. Dewulf, D. Drijvers, H. Van Langenhove, Measurement of Henry's law constant as function of temperature and salinity for the low temperature range, Atmos. Environ. 29 (1995) 323–331. https://doi.org/10.1016/1352-2310(94)00256-K.

[4] J. Dewulf, H. Van Langenhove, P. Everaert, Determination of Henry's law coefficients by combination of the equilibrium partitioning in closed systems and solid-phase microextraction techniques, J. Chromatogr. A. 830 (1999) 353–363. https://doi.org/10.1016/S0021-9673(98)00877-2.

[5] Brand, Transferpette S, BRAND, Wertheim, Germany, n.d. https://shop.brand.de/media/import/1/27/32406/42485/42649/49381/Transferpette_S_2020_EN.pdf.

[6] R.A. Ashworth, G.B. Howe, M.E. Mullins, T.N. Rogers, Air-water partitioning coefficients of organics in dilute aqueous solutions, J. Hazard. Mater. 18 (1988) 25–36. https://doi.org/10.1016/0304-3894(88)85057-X.

[7] P.H. Howard, W.M. Meylan, Handbook of physical properties of organic chemicals, CRC Press, Inc, Boca Raton, The United States of America, 1997.

[8] J.A. Dean, Physical properties, in: Lange's Handb. Chem., 15th ed., McGraw-Hill International, New York, The United States of America, 1999: pp. 373–544. https://doi.org/10.5370/JEET.2015.10.6.2348.

[9] Merck KGaA, Detergents. A guide to the properties and uses of detergents in biological systems, Darmstadt, Germany, 2017. https://www.sigmaaldrich.com/content/dam/sigma-aldrich/1/content/commerce/pdfs/detergents/detergents-guide-mk.pdf.

[10] Kaneka Corporation, KANEKA Surfactin, Osaka, Japan, n.d. https://www.kaneka.co.jp/en/business/qualityoflife/surfactin_catalogue_eng.pdf.

[11] K. Urum, T. Pekdemir, Evaluation of biosurfactants for crude oil contaminated soil washing, Chemosphere. 57 (2004) 1139–1150. https://doi.org/10.1016/j.chemosphere.2004.07.048.

[12] E.J. Gudiña, V. Rangarajan, R. Sen, L.R. Rodrigues, Potential therapeutic applications of biosurfactants, Trends Pharmacol. Sci. 34 (2013) 667–675. https://doi.org/10.1016/j.tips.2013.10.002.

[13] H. Salminen, S. Bischoff, J. Weiss, Formation and stability of emulsions stabilized by Quillaja saponin–egg lecithin mixtures, J. Food Sci. 85 (2020) 1213–1222. https://doi.org/10.1111/1750-3841.15104.

[14] J.T. Davies, A quantitative kinetic theory of emulsion type. I. Physical chemistry of the emulsifying agent, in: Gas/Liquid Liq. Interfaces. Proc. 2nd Int. Congr. Surf. Act., London, England, 1957: pp. 426–438. http://www.firp.ula.ve/archivos/historicos/57_Chap_Davies.pdf.